THE LBNL FEMTOSOURCE (LUX) 10 KHZ PHOTOINJECTOR *

John W. Staples, Steven M. Lidia, Steven P. Virostek, LBNL, Berkeley, California
Robert Rimmer, TJNAF, Newport News, Virginia

Abstract

The LBNL femtosecond-level X-ray source, now christened LUX, a source of hard X-rays with a pulse length in the 50–200 fsec range, will operate at a pulse rate of up to 10 kHz. The room-temperature 1.3 GHz photoinjector includes a modified re-entrant first-cell cavity which minimizes peak surface field, the addition of a third pi-mode acceleration cell, waveguide r.f. feeds to each cell, and an active energy removal procedure which reduces the wall power density of all four cells.

INTRODUCTION

The LUX [1] [2] RF gun will provide nominally a 1–3 nanocoulomb electron bunch, 20 psec long, at a 10 kHz repetition rate from a laser-illuminated Cs_2Te photocathode. The 20 psec beam will be compressed to 2 psec in the first 180 degree arc, and then accelerated to 2.5 GeV, and then through crabbing in the vertical plane, the X-ray pulse from each of a series of undulators will be further optically compressed by means of an asymmetric crystal to as short as 50 fsec.

The resulting photon flux of 10^6 photons per pulse per 0.1% bandwidth up to 12 keV from undulators from the "flat" beam injector to 10^{13} at 20–1000 eV from cascaded harmonic generation in FELs from a future off-axis "round" beam injector results in part from the high 10 kHz pulse rate, which presents a significant challenge for the room-temperature photoinjector. Table 1 lists the important parameters of the 3.5-cell photoinjector.

Table 1: 3.5-Cell Photoinjector Parameters

Parameter	Value	Unit
Frequency	1.3	GHz
Duty Factor	5	percent (equiv)
Cell 1 Q_0	21000	(pure Cu)
Cell 2–4 Q_0	29000	(pure Cu)
Rep Rate	10	kHz
Photocathode Field	64	MV/m
Axial Accel Cell Field	40	MV/m
Charge/bunch	1-3	ncoul
Output Energy	10	MeV

The photoinjector will be immersed in a solenoidal magnetic field to produce a magnetized beam at the photocathode, whose rotational angular momentum will subsequently be converted, through a series of skew quadrupoles, to a "flat" beam with a horizontal-to-vertical emittance ratio of at least 50 to 1. [3] The small vertical beam is then crabbed just before the photon radiators, and the transverse-longitudinal correlation is converted to a time-compressed photon pulse.

The selection of the 10 MeV output energy allows sufficient room for a beam transport system before a 110 MeV 1.3 GHz superconducting accelerator section to provide for emittance compensation solenoids and for the introduction of a septum magnet to combine a future 3.5-cell round-beam photoinjector for driving a future FEL.

Figure 1 shows the 3.5 cell photoinjector embedded in a series of five solenoids. The axial magnetic field at the photocathode is in the 1.0 to 1.5 kGauss range. For a round-beam photoinjector, the solenoids buck the axial B-field at the photocathode.

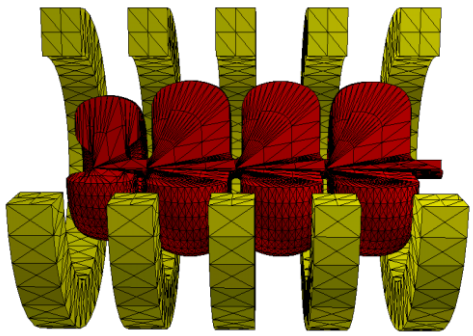

Figure 1: 3.5-Cell Photoinjector and Solenoids

CAVITY FIELD OPTIMIZATION

The first version of the gun was a 2.5-cell structure [4] and subsequently increased to 3.5 cell. With a peak field of 64 MV/m at the photocathode and a 5% duty factor, the peak electric field in the first cell should be held to as low a value as possible, even if it results in a decrease in shunt impedance of the first cell. Increasing radii of curvatures of the cell geometry brought the peak field down from 104 MV/m to 87 MV/m in the nosecone area opposite the photocathode: the ratio of peak to photocathode field was reduced from 1.62 to 1.36, while the peak RF wall current remained at 71 kA/m. The peak RF power demand increased from 580 to 750 kW with this modification.

Figure 2 shows the average wall power density around the surface of a 2-D URMEL calculation of the optimized first cell.

Cells 2 through 4 comprise the three accelerating cells in the photoinjector. The peak axial field in the $\pi/2$ structure

* This work supported by the US Department of Energy under Contract No. DE-AC03-76SF00098.

is 40 MV/m, and the corresponding peak wall field is 46.7 MV/m. The walls are inclined at a 2 degree angle to the perpendicular, and the coupling iris radius is 1 cm.

The asymptotic RF power requirement (several filling times) is 1.35 MW for each cell, but as in the first cell, as described below, the peak available power will be 2.5 MW to fill each cell in 1.5 filling times. As in the first cell, the peak wall power density at the worst case, the outer radius edge of the iris in this case, is 82 $\mathrm{W/cm^2}$.

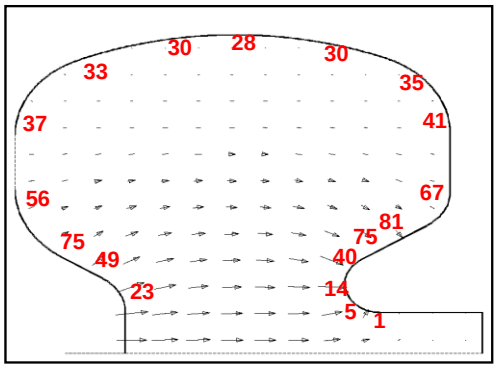

Figure 2: Average wall power density in cell 1 ($\mathrm{W/cm^2}$)

POWER COUPLERS

Each of the four cells is driven by two symmetric iris-coupled waveguides from independent power sources. As described below, due to the 5 microsecond pulse relative to the 3.5 microsecond cavity filling time, the cavities will be overdriven, and then the stored energy will be actively removed to reduce the average power. This will increase the peak fields in the waveguides and iris couplers.

The coupling coefficient is optimized at approximately unity, so $\mathrm{Q_0} \approx \mathrm{Q_{ext}}$ for each of the cavities. The dumbbell-shaped coupling iris area is calculated in the following way: The resonant frequency and $\mathrm{Q_0}$ of the bare cavity are first determined. Using a MAFIA-4[5] half-cell mesh, the problem is set up using a waveguide port model and pinging the cavity with a "soft" packet near the 1.3 GHz resonant frequency. The field decrement is then measured and the iris dimensions are adjusted so that the field decrement per cycle is given by the loaded $\mathrm{Q_L} = \mathrm{Q_0}/2$ for unity coupling.

As the MAFIA-4 mesh is rectangular instead of conformal, fine adjustments will be made to the iris geometry using the *e-mag* module of ANSYS [6], which will also be used to confirm the details of the thermal model for the cavity, particularly in the iris region.

Figure 3 shows the MAFIA-4 half-model of the first cell with coupling port. The first $\lambda/4$ section of the waveguide is half-height, to make room for the solenoids, which straddle the intercell boundary regions.

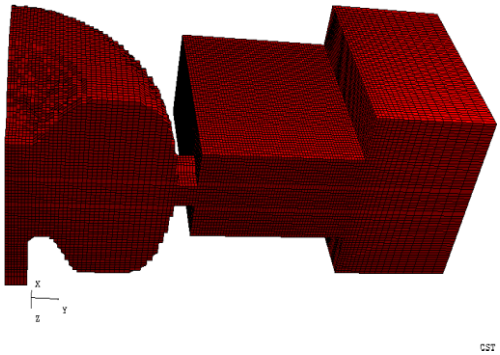

Figure 3: MAFIA-4 Mesh of Cell1 and Waveguide Coupler

REDUCING AVERAGE WALL POWER

With unity coupling, the filling time of each cell is on the order of 3.5 microseconds. At a 10 kHz repetition rate and 5 microsecond pulse length, the macroscopic duty factor is 5%, and at 5 microseconds, only 1.5 filling times have occurred. For short RF pulse lengths, the "square pulse" analysis is inadequate to address the thermal dissipation. Extending the pulse length will further increase the already high duty factor, and overvolting the cavity will increase the average power dissipation, which would already be 75 kW per accelerating cell.

The field will rise to 77% of full at 1.5 filling times, so overpowering each cell by $1/0.77^2$, or about 2.5 MW, including a realistic value for the cavity Q_0 and waveguide and circulator losses will achieve operating gradient at 5 microseconds (the beam pulse is 20 psec). The average power may be reduced by about 40% by reversing the drive phase ("reverse SLEDding") and actively removing the stored energy to the circulator dummy load.

Figure 4 shows the cavity field level without and with active energy removal. The cavity is overdriven for 5 microseconds. Then the drive phase is reversed and drive power continues for about another 2 microseconds until the cavity is empty. (The beam loading is insignificant.)

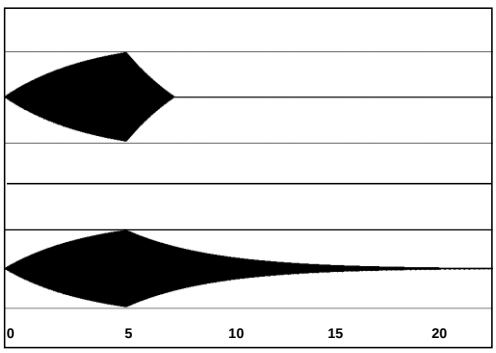

Figure 4: Fields in Cavity without and with phase flip at 5 microseconds. Horizontal scale: time in microseconds, Vertical scale: fields in cavity with and without active energy removal.

Peak Temperature Rise

Even though the peak wall power density approaches 82 $\mathrm{W/cm^2}$ at one point, the average wall temperature will be less than 30 C above the wall temperature in the cooling channel (plus the film temperature difference). The Laplace thermal diffusion equation $k\nabla^2 T + \dot{Q} = \rho C_v \dot{T}$ is integrated in one dimension, with specific heat C_v, thermal conductivity k and target density ρ characteristic of copper for a 1 cm thickness between cavity surface and cooling channel. For a wall current density of 70 kA/m, 5 microsecond pulses at a 10 kHz rate, the asymptotic temperature rise is 30.3 C. Figure 5 shows the results of the beginning of the integration, before asymptopia, of the temperature rise for each 5 microsecond pulse of 0.6 C.

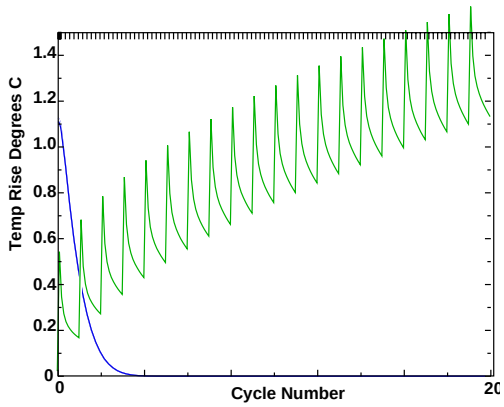

Figure 5: Temperature rise each cycle of worst-case wall power density, the first 20 cycles. Asymptote is 30.3 C

BEAM DYNAMICS

The proposed LUX photoinjector gun design will deliver a beam of quality similar to that of other operating RF guns. The brightness for the LUX RF gun is based upon a 1 nanocoulomb bunch with 3π mm-mrad normalized RMS emittance. This brightness is conservative, and is similar or less than that achieved at the same frequency from TTF and AFEL guns, for example.

The detailed beam dynamics in the RF gun and injector have been studied using the particle tracking code ASTRA [7]. For the flat beam injector, a magnetized cathode produces a finite canonical angular momentum carried by the beam. The 4D phase space, described in terms of horizontal and vertical coordinates and momenta is coupled. A decoupled description can be obtained if one is willing to use "drift" and "cyclotron" coordinates [8]. These normal mode coordinates each have an associated emittance. The product of the drift and cyclotron emittances is the total 4D emittance of the beam. For linear forces, the 4D emittance is preserved along the beamline. The variation of the different emittances through the RF gun and subsequent drift are shown in Figure 6. The photocathode is located at z = 0 meters. Shown are the cyclic mode (drift, cyclotron), total 4D, and usual radial RMS normalized emittances, along with the RMS horizontal spot size.

A discussion of injector optimization, emittance compensation, and dual-injector operation can be found in a companion paper at this conference [9].

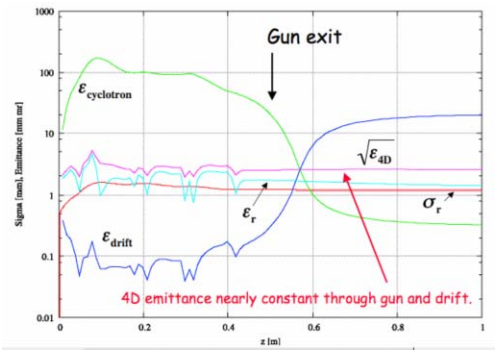

Figure 6: Evolution of Radial and Transverse Emittance

REFERENCES

[1] J. N. Corlett at al, "Feasibility Study for a Recirculating Linac-Based Facility for Femtosecond Dynamics", LBNL formal report LBNL-51766, Dec 2002.

[2] J. N. Corlett et al, "A Recirculating Linac-Based Facility for Ultrafast X-ray Science", this conference.

[3] D. Edwards et al., "The Flat Beam Experiment at the FNAL Photoinjector", Proc. XXth International Linac Conference, Monterey, 2000

[4] R. A. Rimmer, et al, "A High-Gradient High-Duty-Factor RF Photo-Cathode Electron Gun", 2002 EPAC, Paper TUPRI040, Paris, 2002

[5] Gesellshaft für Computer Simulationstechnik, Lauteschlägerstraße 38, D-64289 Darmstadt, Germany

[6] ANSYS Finite Element Analysis Code, Release 7.0, SAS IP, Inc., Canonsburg, PA.

[7] K. Flöttmann, ASTRA User Manual, DESY, 2000. The program and its documentation can be obtained at the web site www.desy.de/∼mpyflo

[8] see, for example, A. Burov, S. Nagaitsev, and Y. Daroslav Phys. Rev. E 66, 016503 (2002)

[9] S. Lidia, et. al., An injector for the proposed Berkeley ultrafast x-ray light source, this conference,WPAB021